

A Simplified Model for Mechanical Loads under Angular Misalignment and Unbalance

Úrsula B. Ferraz, Paulo F. Seixas, and Webber E. Aguiar

Abstract—This paper presents a dynamic model for mechanical loads of an electric drive, including angular misalignment and including load unbalance. The misalignment model represents the effects of the universal joint between the motor and the mechanical load. Simulation results are presented for an induction motor driving a mechanical load with angular misalignment for both flexible and rigid coupling. The models presented are very useful in the study of mechanical fault detection in induction motors, using mechanical and electrical signals already available in a drive system, such as speed, torque and stator currents.

Keywords—Angular misalignment, fault modeling, unbalance, universal joint.

I. INTRODUCTION

MECHANICAL failures are the leading causes of downtime in industrial electric drive systems. The unbalance and the misalignment are the most frequent causes of these problems [1]-[3]. In this context, the detection of these faults at an early stage in induction motors are of paramount importance due to its wide use in industrial plants [4].

The aim of this paper is to present a simple and effective model of two faults: angular misalignment between motor and mechanical load and load imbalance.

The model for angular misalignment is based on the universal joint effect. Both models describe only the tangential forces without attempting to describe the radial force components, which are responsible for the mechanical vibration.

The modeling of mechanical faults is complex for diverse aspects, as the complex machine geometry and the difficulty to isolate a specific fault problem from the others [5].

In [6] a rotor-bearing system is modeled to include the coupling misalignment forces and moments, in a high order finite element of eight degrees of freedom per node. In [1], Xu and Marangoni generalized the equations of motion for a complete motor - flexible coupling - rotor system using the component mode synthesis method. The universal joint effect is included in the model to take the misalignment into account. In both cases, it is shown that the angular misalignment introduces terms at twice the rotational frequency in the

signals spectrum, and [1] shows that load unbalance introduces terms at rotational frequency.

II. THE UNIVERSAL JOINT MODEL

The diagram of an universal joint is presented in Fig. 1. The drive shaft forms an angle β with the load shaft. This shaft rotates at a speed ω_1 and its angular position is θ . The load shaft rotates at speed ω_2 and its angular position is Φ .

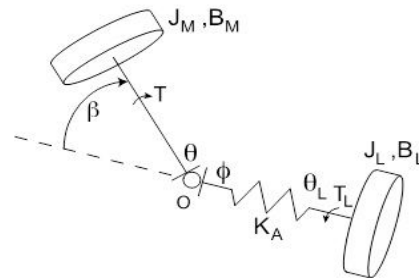


Fig. 1 Universal joint diagram

The angular displacements of motor and load shafts are related by (1).

$$tg(\theta) = \frac{tg(\Phi)}{\cos(\beta)} \quad (1)$$

The relationship between the two shafts speeds can be derived from (1) and is given by (2).

$$\frac{\omega_1}{\omega_2} = \frac{1 - \sin^2(\beta)\sin^2(\theta)}{\cos(\beta)} = g(\theta) \quad (2)$$

This equation can be rewritten as (3).

$$\frac{\omega_1}{\omega_2} = \frac{1 + \cos^2(\beta)}{2\cos(\beta)} + \frac{1 - \cos^2(\beta)}{2\cos(\beta)} \cos(2\theta) = K_1 + K_2 \cos(2\theta) \quad (3)$$

Since the mechanical power is the same in both sides ($T_1\omega_1 = T_2\omega_2$) the torques relationship is given by (4).

$$\frac{T_1}{T_2} = \frac{1}{g(\theta)} \quad (4)$$

It is observed from the above equations that, although the two shafts rotate at the same average speed, their instantaneous velocities are different. Equation (3) shows the

U. B. Ferraz is with the Federal University of Minas Gerais (UFMG), MG, Brazil (e-mail: ursula.b.ferraz@gmail.com).

P. F. Seixas is the Federal University of Minas Gerais (UFMG), MG, Brazil (e-mail: paulos@cpdee.ufmg.br).

W. E. Aguiar is with Energy Company of Minas Gerais (CEMIG), MG, Brazil.

presence of a term at twice the frequency of motor rotation. The amplitude of this term, K_2 , increases with increasing misalignment angle.

For low values of angular misalignment $g(\theta) \approx 1$, the torques ratio, $1/g(\theta)$ can be approximated by a Taylor series expansion around $g(\theta) = 1$, which gives:

$$\frac{1}{g(\theta)} \approx 2 - g(\theta) = \frac{4\cos(\beta) - \cos^2(\beta) - 1}{2\cos(\theta)} - \frac{1 - \cos^2(\beta)}{2\cos(\beta)} \cos(2\theta) \quad (5)$$

From (5), it can be noted that the torques ratio consists of a constant term and an oscillating term at twice the frequency of rotation just like the speed ratio. The amplitude of this term is the same of the speed ratio.

III. MECHANICAL LOAD DYNAMIC MODEL INCLUDING ANGULAR MISALIGNMENT

With the model of universal joint established, the dynamic model of load and coupling including angular misalignment can be deduced. In the present study, both rigid and flexible coupling are considered. The mechanical equivalent circuit for rigid coupling is shown in Fig. 2.

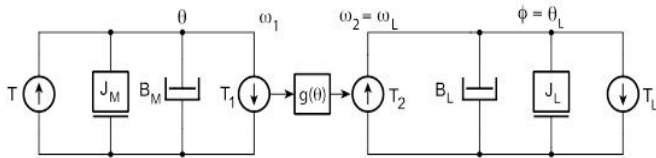


Fig. 2 Rigid coupling – equivalent mechanical circuit

where J_M and B_M are the inertia and the dynamic friction coefficient of the motor, and J_L and B_L are the inertia coefficient and the dynamic friction coefficient of the load, respectively. T and T_L are respectively the motor and the load torques. The universal joint effect is included in the circuit as a non-linear gear train with transfer ratio $g(\theta)$.

Considering the differential equations of the mechanical circuit of Fig. 2 and the universal joint equations, the mechanical load equation including angular misalignment is:

$$T = (J_M g(\theta) + \frac{J_L}{g(\theta)}) \frac{d\omega_L}{dt} + (B_M g(\theta) + \frac{B_L}{g(\theta)}) \omega_L + \frac{T_L}{g(\theta)} - 2K_2 J_M \sin(2\theta) \omega_1 \omega_L \quad (6)$$

The resulting differential equation is time variant. The load torque reflected on the motor shaft includes oscillations at twice the frequency of rotation, as predicted by the universal joint model. The last term in (6) also oscillates at twice the rotation frequency and its amplitude varies with the multiplication of velocities.

For flexible coupling, the equivalent mechanical circuit is given by Fig. 3, where K_A is the flexible coupling elasticity constant, which can be obtained from the manufacturer's datasheets.

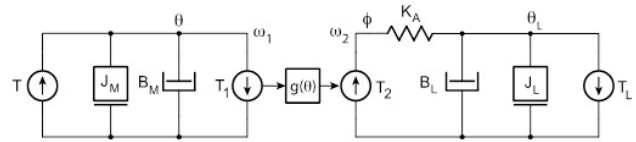


Fig. 3 Flexible coupling – equivalent mechanical circuit

The differential system equations are given by (7) to (10).

$$T = J_M \frac{d\omega_1}{dt} + B_M \omega_1 + T_1 \quad (7)$$

$$\omega_1 = \frac{d\theta}{dt} \quad (8)$$

$$T_2 = K_A(\Phi - \theta) = J_L \frac{d\omega_L}{dt} + B_L \omega_L + T_L \quad (9)$$

$$\omega_L = \frac{d\theta_L}{dt} \quad (10)$$

IV. THE UNBALANCE MODEL

The imbalance can occur in several ways [7]. In this modeling, it was considered that the static imbalance is located in a plane perpendicular to the axis of rotation. The static imbalance is defined as the condition in which the mass axis is parallel displaced of rotation axis. It is called static because, even with the power off, the extra weight causes the rotor to rotate to position the point of greatest weight down, allowing easily detect the existence of such imbalance.

The unbalance is caused by a mass "m" punctiform located at a distance "r" from the axis, as shown in Fig. 4.

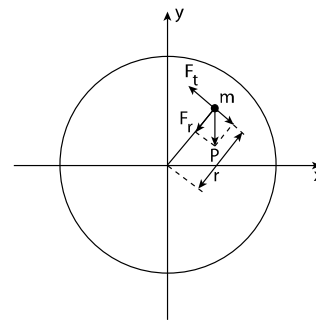


Fig. 4 Model for static unbalance

The tangential component of the weight is given by:

$$F_t = -mg \cos(\theta) \quad (11)$$

The torque due to this tangential force is given by:

$$T_t = r F_t = mgr \cos(\theta) \quad (12)$$

This result is in accordance with [8] which states that the unbalanced torque introduces a term in the load oscillating at a frequency of rotation.

We now include this model in dynamic equations of the motor and associated load, as (13) and (14). In the

expressions, T is the electromagnetic torque, T_L , the torque load, J_M and J_L are the coefficients of inertia of the motor and load, respectively, and J_m is the coefficient of inertia m , responsible for the imbalance ($J_m = mr^2$). The coefficients of viscous friction of the motor and load are, respectively, B_M and B_L .

$$T = (J_M + J_L + J_m) \frac{d\omega}{dt} + (B_M + B_L)\omega + T_L + m g r \cos(\theta) \quad (13)$$

$$\omega = \frac{d\theta}{dt} \quad (14)$$

V. RESULTS

A Matlab script was developed for the simulation of an induction motor driving a constant torque load, including a coupling with angular misalignment. The induction motor parameters are included at the appendix.

The results for rigid coupling with an angular misalignment of one degree ($\beta = 1^\circ$) are shown in Figs. 4 to 11.

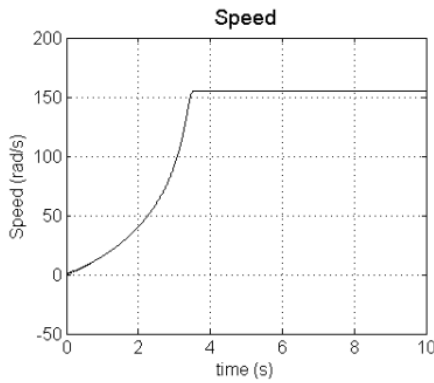


Fig. 4 Speed

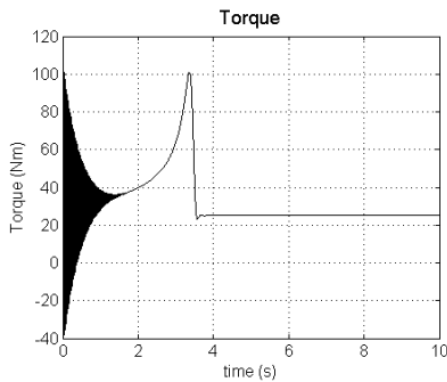


Fig. 5 Torque

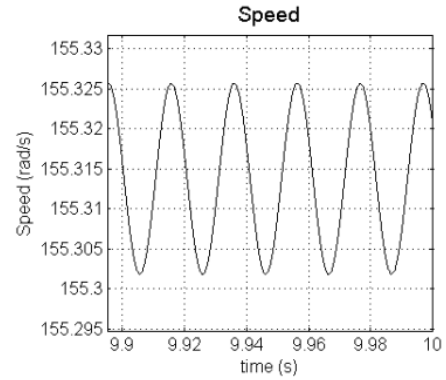


Fig. 6 Speed: zoom at steady state

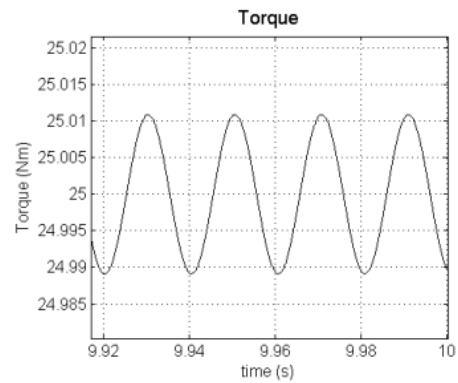


Fig. 7 Electromagnetic torque: zoom at steady state

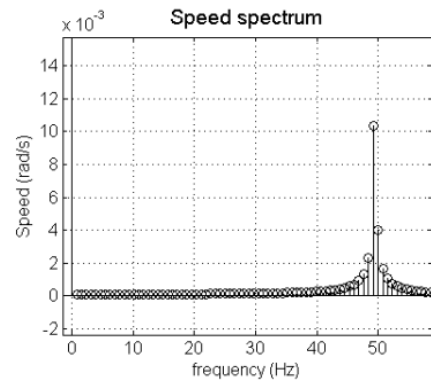


Fig. 8 Speed frequency spectrum with zoom in the fault frequency

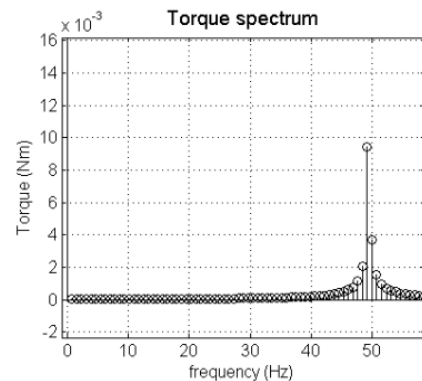


Fig. 9 Torque frequency spectrum with zoom in the fault frequency

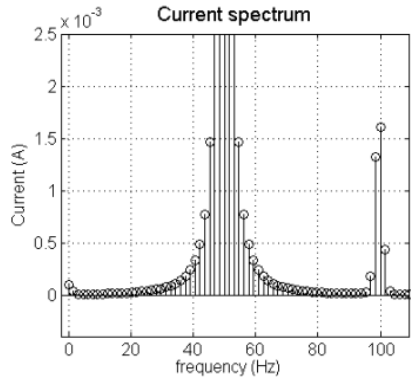


Fig. 10 Current frequency spectrum with zoom in the fault frequency plus supply frequency

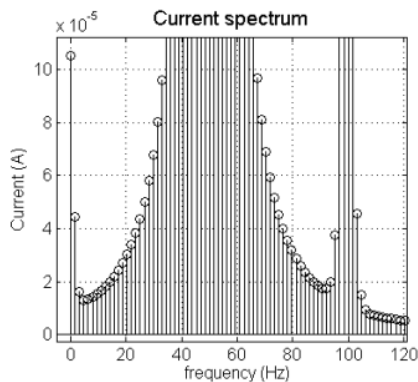


Fig. 11 Current frequency spectrum with zoom in the fault frequency minus supply frequency

It is important to observe that there are fluctuations in electromagnetic torque and speed at steady state. Figs. 8 to 11 shows the frequency spectrum of torque, speed and current signals. The frequency of those oscillations into torque and speed signals are 49.4 Hz, as expected for a 4 poles machine, feed directly by 50Hz means. In the current signal of misalignment, the frequency components appear in $f_s \pm f_f$, where f_s is the supply frequency and f_f is the frequency of fault. In angular misalignment, the frequency of fault corresponds to two times the rotational frequency. These results correspond to the expected values, described on the references [9]-[11].

The amplitude of torque oscillations is 0,011Nm which corresponds to 440 ppm of the nominal torque and the amplitude of speed oscillations is 0,0125 rad/s, or 80 ppm of the average speed at steady state.

For a flexible coupling with an elasticity coefficient $KA = 1289.155$ and angular misalignment of one degree ($\beta=1^\circ$), the results are shown in Figs. 12 to 19.

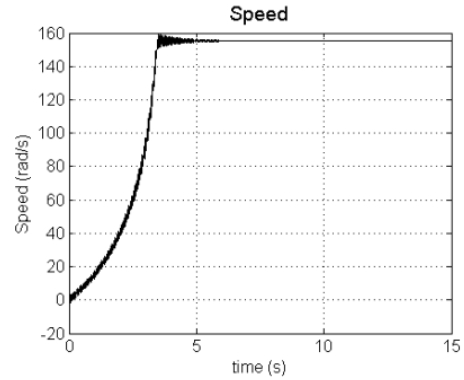


Fig. 12 Speed

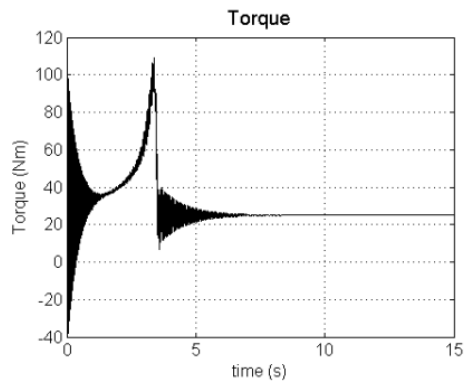


Fig. 13 Torque

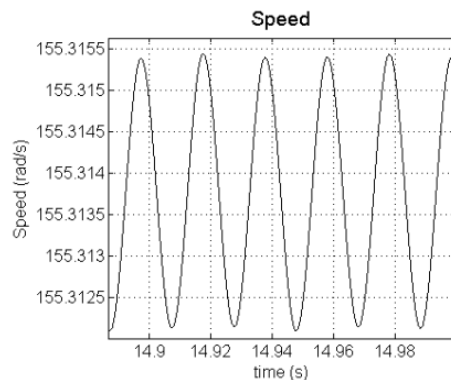


Fig. 14 Speed: zoom at steady state

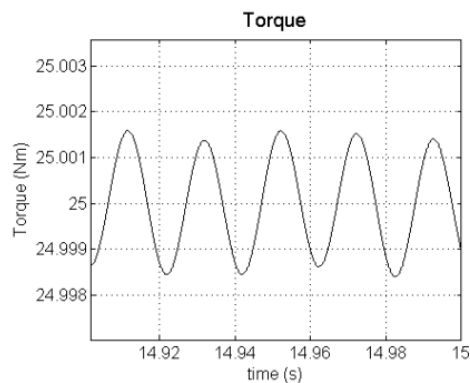


Fig. 15 Torque: zoom at steady state

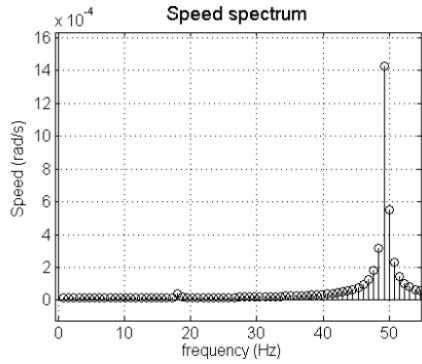


Fig. 16 Speed frequency spectrum with zoom in the fault frequency

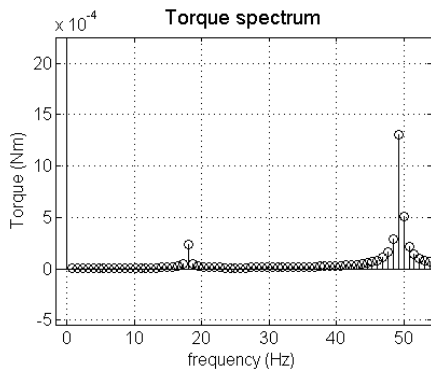


Fig. 17 Torque frequency spectrum with zoom in the fault frequency

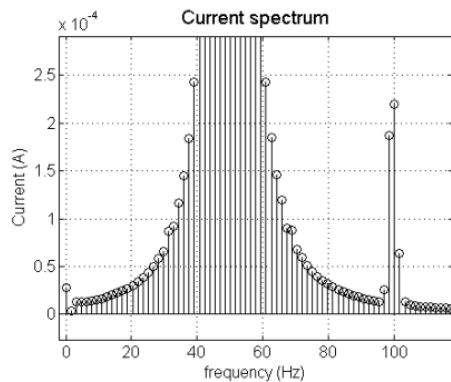


Fig. 18 Current frequency spectrum with zoom in the fault frequency plus supply frequency

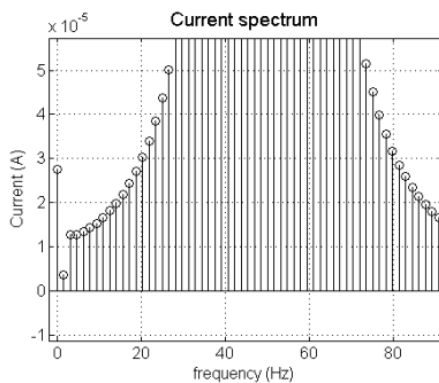


Fig. 19 Current frequency spectrum with zoom in the fault frequency minus supply frequency

TABLE I
 OSCILLATIONS VALUES FOR ANGULAR MISALIGNMENT

	Rigid Coupling		Flexible Coupling	
	$\beta=1^\circ$	$\beta=3^\circ$	$\beta=1^\circ$	$\beta=3^\circ$
Torque (Nm)	0,01	0,1	18×10^{-4}	0,013
Speed (rad/s)	$12,5 \times 10^{-3}$	0,105	0,002	0,015

It is observed in these figures, fluctuations in torque and speed during the starting transient, greater than with rigid coupling. It can be concluded that the insertion of an elastic constant in the coupling model makes the dynamic response of the system slower and more oscillatory. The amplitude of torque oscillations at steady state is 0,0018Nm which corresponds to 72 ppm of the nominal torque and the amplitude of speed oscillations is 0,002 rad/s, or 13 ppm of the average speed at steady state.

Simulations were also carried out with angular misalignment of 3 degrees and a summary of all results appears in Table I.

In Figs. 21 to 27 are shown the simulation results for a load imbalance caused by a mass of 10g to 28cm from the rotation axis, which corresponds to an imbalance of 28×10^{-4} kg.m.

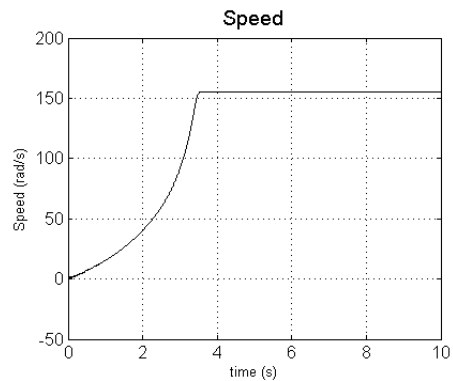


Fig. 21 Speed

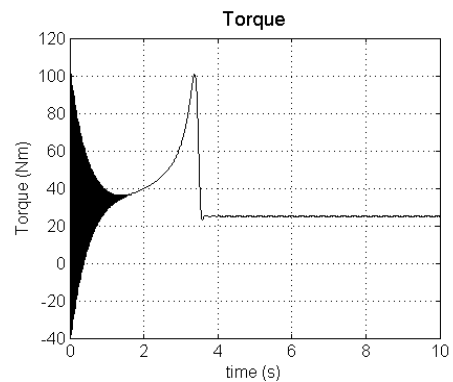


Fig. 22 Torque

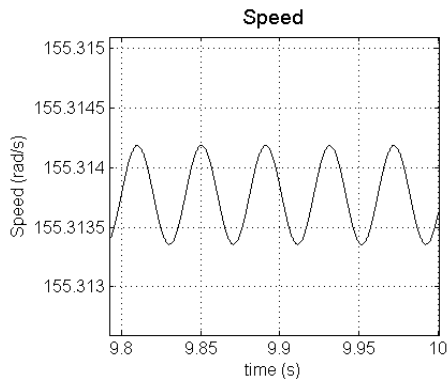


Fig. 23 Speed: zoom at steady state

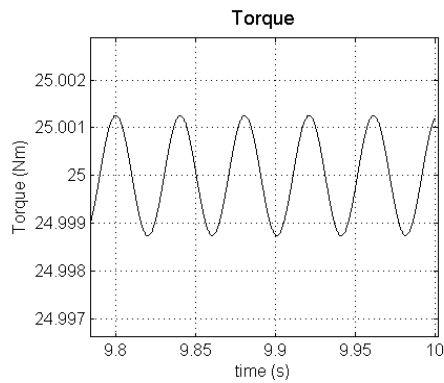


Fig. 24 Torque: zoom at steady state

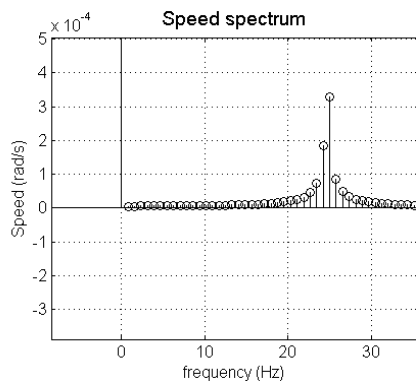


Fig. 25 Speed frequency spectrum with zoom in the fault frequency

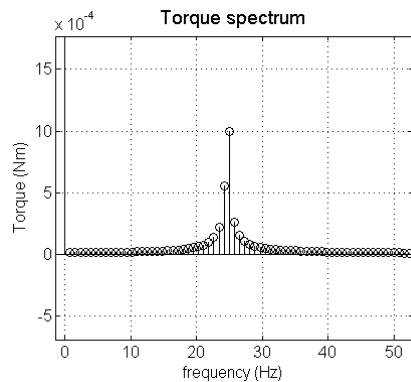


Fig. 26 Torque frequency spectrum with zoom in the fault frequency

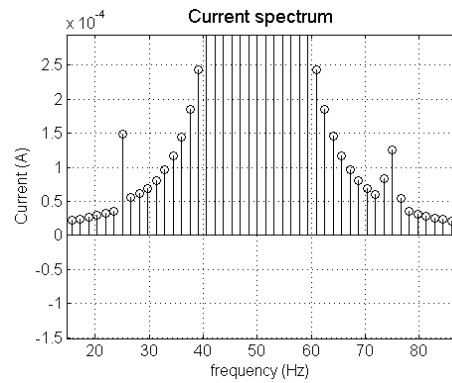


Fig. 27 Current frequency spectrum with zoom in the fault frequency around supply frequency

VI. CONCLUSION

It can be observed that the oscillations of torque and speed in steady state with rigid coupling are greater than with flexible coupling. Nevertheless, the oscillations with flexible couplings are higher in the transient response. It is also observed that the steady state oscillations increase substantially (almost 10 times) with the increasing of only two degrees in the misalignment angle for both rigid and flexible coupling.

TABLE II
 MOTOR PARAMETERS

Parameter	Value
Stator resistance	0,95 Ω
Rotor resistance	0,36 Ω
Magnetic inductance	0,122 H
Stator leakage inductance	0,0047 H
Rotor leakage inductance	0,0047 H
Inertia	0,2225 kg.m ²
Number of poles	4
Nominal Power	5,5 kW
Nominal Frequency	50 Hz
Nominal Voltage	380 V

These results demonstrate the ability of the model to represent the dynamic model of the load including the angular misalignment. The model can represent rigid or flexible couplings. It can be used to study mechanical faults in induction motors by analyzing electrical and mechanical variables, such as, current and speed. The model shows the ability to induce the expected results in the frequency spectrum even in the electrical variable, what is very useful in fault detection.

ACKNOWLEDGMENT

U.B.F thanks the teacher Paulo Seixas and teachers of Power Electronic Department at Federal University by all support given in the research.

We thank CEMIG (Energy Company of Minas Gerais) the

financial support to the research.

REFERENCES

- [1] M. Xu and R.D. Marangoni, "Vibration Analysis Of A Motor-flexible Coupling-Rotor System Subject To Misalignment And Unbalance, Part I: Theoretical Model and Analysis", *Journal of Sound and Vibration*, Volume 176, Issue 5, 6 October 1994, Pages 681-691.
- [2] T.H. Patel, and A.K. Darpe, "Experimental investigations on vibration response of misaligned rotors." In: *Mechanical Systems and Signal Processing*, Volume 23, Issue 7, October 2009, Pages 2236-2252.
- [3] A. Kr. Jalan and A.R. Mohanty, "Model based fault diagnosis of a rotor-bearing system for misalignment and unbalance under steady-state condition." In *Journal of Sound and Vibration*, Volume 327, Issues 3-5, 13 November 2009, Pages 604-622.
- [4] M.E.H. Benbouzid and G.B. Kliman, "What stator current processing-based technique to use for induction motor rotor faults diagnosis?" In: *Transactions on Energy Conversion*, , vol.18, no.2, pp. 238- 244, June 2003.
- [5] M. Tsypkin, "Induction motor condition monitoring: Vibration analysis technique - A practical implementation." In: *Electric Machines & Drives Conference (IEMDC)*, 2011 IEEE International , vol., no., pp.406-411, 15-18 May 2011.
- [6] A.S. Sekhar, B.S. Prabhu, "Effects of coupling misalignment on vibrations of rotating machinery." In: *Journal of Sound and Vibration*, Volume 185, Issue 4, 31 August 1995, Pages 655-671.
- [7] H.P.Bloch, F.K.Geitner , *Balancing of machinery components*. In: Bloch, H.P.; Geitner ,F.K. *Practical Machinery Management for Process Plants*, Gulf Professional Publishing, 2005, Volume 3, Pages 258-366.
- [8] C. Kral, T.G.Habetler, R.G. Harley, Detection of mechanical imbalances of induction machines without spectral analysis of time-domain signals. In: *Industry Applications*, IEEE Transactions on , vol.40, no.4, pp. 1101- 1106, July-Aug. 2004.
- [9] J.M. Bossio, G.R. Bossio and C.H. De Angelo, "Angular misalignment in induction motors with flexible coupling." In: *Industrial Electronics, 2009. IECON '09. 35th Annual Conference of IEEE* , vol., no., pp.1033-1038, 3-5 Nov. 2009.
- [10] R.R. Obaid, T.G. Habetler and R.M. Tallam, "Detecting load unbalance and shaft misalignment using stator current in inverter-driven induction motors." In: *Electric Machines and Drives Conference, 2003. IEMDC'03. IEEE International*, vol.3, pp. 1454- 1458 vol.3, 1-4 June 2003.
- [11] R.R. Obaid, T.G. Habetler and D.J. Gritter, "A simplified technique for detecting mechanical faults using stator current in small induction motors." In: *Industry Applications Conference, 2000. Conference Record of the 2000 IEEE*, vol.1, no., pp.479-483 vol.1, 2000.